IOP Conf. Series: Journal of Physics: Conf. Series **847** (2017) 012059 doi:10.1088/1742-6596/847/1/012059

# The potential of polymer gel dosimeters for 3D MR-IGRT quality assurance

**Y Roed[1,2], Y Ding[3], Z Wen[2], J Wang[2], L Pinsky[1] and G Ibbott[2]**
[1]Department of Physics, University of Houston, Science and Research Building 1, 3507 Cullen Blvd. Houston, TX 77204 USA
[2]Department of Radiation Physics, University of Texas MD Anderson Cancer Center, 1400 Pressler St., Houston, TX 77030 USA
[3]Department of Imaging Physics, University of Texas MD Anderson Cancer Center, 1400 Pressler St., Houston, TX 77030 USA

Email: gibbott@mdanderson.org

**Abstract**. Advances in radiotherapy technology have enabled more accurate delivery of radiation doses to anatomically complex tumor volumes, while sparing surrounding tissues. The most recent advanced treatment modality combines a radiation delivery system (either Cobalt-60 therapy heads or linear accelerator) with a diagnostic magnetic resonance (MR) scanner to perform MR-image guided radiotherapy (MR-IGRT). For a radiation treatment plan to be delivered successfully with MR-IGRT the compliance with previously established criteria to validate the passing of such plans has to be confirmed. Due to the added strong magnetic field a new set of quality assurance standards has to be developed. Ideal detectors are MR-compatible, can capture complex dose distributions and can be read out with MRI. Polymer gels were investigated as potential three dimensional MR-IGRT quality assurance detectors.

## 1. Background

Image-guided radiotherapy (IGRT) is currently considered the standard in radiotherapy for treating cancer patients and is achieved by integrating on-board imaging devices with linear accelerators [1]. Patients are positioned for each treatment fraction with on-board imagers using bony anatomy and corrections may be made during the treatment itself to allow for more accurate dose delivery to the tumor while limiting the dose to the surrounding normal tissue. Quality assurance (QA) standards have been developed to ensure the precision of prescribed radiation treatment plans. Only a few millimeters deviation between the treatment plan and the actual delivered treatment is accepted for the plan to pass. These rigorous passing criteria lead to more accurate treatment delivery [2].

Magnetic resonance-image guided radiotherapy (MR-IGRT) has been proposed as an advanced treatment modality. Delineation of the tumor and adjacent organs is improved by the superior soft tissue contrast available from MR images. With the presence of a strong magnetic field, Lorenz forces act on secondary electrons influencing the shape of the delivered dose distribution in three dimensions. It remains essential to confirm that the delivered dose complies with the treatment plan within strict passing criteria. QA standards for treatment plan verification for MR-IGRT delivery systems are presently being developed. The strong magnetic field adds new challenges in the selection of QA dosimeters as electronic detectors need to be MR-compatible and their response might be influenced under such conditions.

Polymer gel dosimeters have previously been shown to be a useful tool to capture complex 3D dose distributions with steep dose gradients [3, 4]. The polymerization of the gel in response to radiation dose can be measured with an MR scanner because spin-spin relaxation rates (R2) increase in proportion to radiation dose [3, 5]. These properties make them favorable devices for QA standards in MR-IGRT.

The influence of strong magnetic fields on the steep dose gradients of radiation fields was investigated. Polymer gel dosimeters were irradiated with two different delivery systems for which different magnetic field strengths and radiation field sizes were used. This choice resulted from limited availability of one of the delivery systems. Results from exposures of the polymer gels are presented in this study.

## 2. Methods

Custom-designed glass cylinders filled with a proprietary polymer gel mixture were provided by the manufacturer (MGS Research, Madison, Connecticut). Each dosimeter consisted of a cylindrical sensitive volume (4 cm height, 5 cm diameter) that was attached to a 10 cm long filling port intended to minimize oxygen perfusion into the sensitive volume.

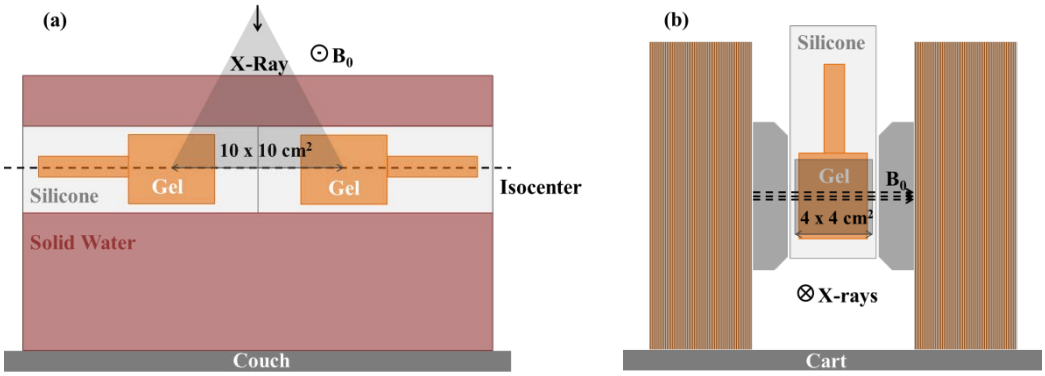


**Figure 1**. Experimental setup for (a) MR-Linac and (b) electromagnet combined with Versa HD™

A set of dosimeters was irradiated with a non-clinical MR-Linac pilot system (Elekta AB, Stockholm, Sweden) that combined a 1.5 T Philips Marlin MR scanner with a 7 MV linear accelerator (MR-Linac). The dosimeters were placed separately in a phantom to assure full scatter conditions and irradiated to 15 Gy. The center of each dosimeter was positioned at isocenter distance in the penumbra region of a 10x10 $cm^2$ radiation field to capture the field edges parallel to the magnetic field lines (Figure 1 a).

The experiment was repeated with the dosimeters placed in a 1.04 T magnetic field generated by an electromagnet (GMW Associates, San Carlos, California) and irradiated with a 6 MV linear accelerator (Elekta Versa HD™). A dose of 10 Gy was delivered to the sensitive volume. A source-to-axis-distance of 300 cm was used to avoid interference with the linear accelerator. At this distance the radiation field was collimated to 4x4 $cm^2$ to shield the electromagnet (Figure 1 b). The setup in the MR-Linac was reproduced, in that the X-ray beam, the magnetic field lines and the profiles were all perpendicular to each other.

All dosimeters were imaged with a 3T scanner (GE Discovery™ MR750, Waukesha, Wisconsin) 24h after irradiation using a 2D spin echo sequence with a repetition time of TR = 1000 ms and four variable echo times TE = 10, 20, 60, and 100 ms.

R2 maps were generated for all dosimeters and 18 line profiles across the sensitive volume were averaged. A Savitzky-Golay filter with window length M = 11 and polynomial order N = 3 was applied to the averaged R2 values to smooth the profiles. After smoothing, the data were normalized and the inflection point was determined for either side of the radiation field from which 80/20 penumbra widths were obtained. Data obtained with the MR-Linac were compared with measurements with

Gafchromic™ EBT3 film of the cross-plane profile of the 10x10 $cm^2$ field from the MR-Linac, under the same conditions.

The directions of the X-ray beam, the magnetic field and the line profile are described in the International Electrotechnical Commission gantry coordinate system, which rotates with the gantry. In this case, the beam is always directed toward $-Z_g$, the magnetic field lines appear to be pointing parallel to the $+Y_g$ axis while the MR scans have been performed parallel to the $X_g$ axis.

## 3. Results

The penumbra regions of the radiation field were clearly visible in all dosimeters. The application of the Savitzky-Golay filter to the averaged line profiles smoothed the data. The line profiles across the penumbra regions showed the distinct shape of the beam profile arising from the influence of the Lorentz force on secondary electrons in the presence of the magnetic field. The Lorentz force preferentially directs secondary electrons in the $+X_g$ direction when the magnetic field lines point in the $+Y_g$ direction and the gantry is at 0 degree with the X-ray beam in the $-Z_g$ direction. The field edge corresponding to the $-X_g$ of the radiation field appeared more rounded. The absence of quasi-electronic equilibrium in the $-X_g$ penumbra of the radiation field prevented replacement of the electrons that were swept from the penumbra region into the field. On the $+X_g$ side of the field, however, a sharper penumbra appeared as secondary electrons were deflected out of the radiation field while a quasi-electronic equilibrium present inside the field replaced electrons generated in the penumbra region.

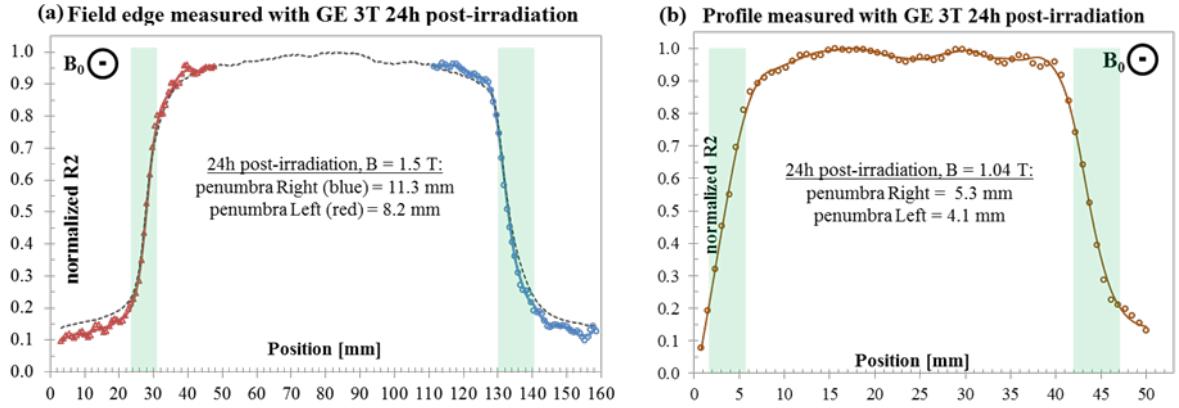


**Figure 2.** Averaged (circles) and smoothed (solid line) line profiles measured when irradiated with the MR-Linac (a) and with the Versa HD™ and electromagnet (b); film measurements of the cross-plane profile (dashed line) from the MR-Linac are shown for comparison.

The averaged (circles) and smoothed (solid line) line profiles across the penumbra region measured with the MR-Linac are shown in Figure 2 a. Due to their size the dosimeters did not cover the full radiation field and the field size (the distance between inflection points) was not demonstrated with this setup. The two transition regions from outside to fully inside the radiation field were visualized on R2 gray scale maps Line profiles across the regions indicated the distinct shape of the field edges in the presence of the magnetic field and agreed well with the cross-plane film profile (dashed line). The fall-off of the right field edge ($+X_g$) appeared steeper than the fall-off on the left ($-X_g$). The 80/20 penumbra regions are indicated by shading in Figure 2 a. The penumbra width on the right was determined to be 11.3 mm on the right and 8.2 mm on the left.

The collimated 4x4 $cm^2$ radiation field was fully captured inside the sensitive volume of the dosimeters when using the electromagnet in combination with the Versa HD™ linear accelerator as seen in Figure 2 b. However, the tails of both field edges fell outside the sensitive volume. Although the Savitzky-Golay filter smoothed the data, some fluctuations remained. The distinct shape of the beam profile due to the presence of the magnetic field was evident. The transition regions on R2 gray scale maps appeared to be very similar in width. Calculations confirmed this observation: the penumbra on

the left ($-X_g$) measured 4.1 mm while the penumbra on the right ($+X_g$) was 5.3 mm wide. The distance between the inflection points was 40.6 mm. The shading in Figure 2 b indicates the penumbra regions.

## 4. Discussion and Conclusions

The results showed that the polymer gel dosimeters could capture and resolve the steep dose gradients of penumbra regions of radiation fields in the presence of magnetic fields of different strengths. Smoothing the data with a Savitzky-Golay filter decreased the noise across the transition region so that the inflection point could be determined and the widths of the penumbrae could be calculated.

Investigations of field edges parallel to the magnetic field lines have been performed previously by irradiating polymer gels with an MR-Linac [6] and with Monte Carlo simulations [7]. Similar differences in penumbra width for the $-X_g$ and $+X_g$ field edges were obtained when applying a sigmoidal fit to measured data to calculate penumbra widths. The Monte Carlo study showed the same distinct shape of the penumbrae demonstrated by profiles drawn perpendicularly to the magnetic field lines.

The number of R2 values measured was defined by the MR scanner resolution and the selection of scanning parameters (matrix size, field of view). A high spatial resolution introduced noticeable noise in the MR images resulting in noisy profiles. To adequately determine penumbra widths the noisy data were smoothed. With a pixel size of 0.8 mm the differences in calculated penumbra widths fell within the dimensions of a few pixels.

Considering the difficulty of set up in the electromagnet at the extended distances and the MR scanner resolution the measured field size agreed well with the collimated field size. Using different or more optimized parameters for the Savitzky-Golay filter might improve the noise reduction after applying the filter.

This study demonstrated great promise of using polymer gels as relative 3D quality assurance devices for testing radiation treatment plans delivered by MR-IGRT delivery systems**.** More studies are needed to extend the set of measurements to include more geometrically complex dose distributions through delivery of intensity modulated radiotherapy treatment plans.

## 5. References

[1] Greer P B *et al* 2007 *Med. Phys*. **34** 4389-98
[2] Ezzell G A *et al* 2009 *Med. Phys* **36** 5359-73
[3] Baldock C *et al* 2010 *Phys. Med. Biol*. **55** R1-63
[4] Ibbott G S *et al* 1997 *Int. J. Radiation Oncology Biol. Phys.* **38** 1097-103
[5] De Deene Y *et al* 1998 *Radiotherapy and Oncology* **48** 283-91
[6] Roed Y *et al* 2016 *Med. Phys.* **43** 3661
[7] Raaymakers B W *et al* 2004 *Phys. Med. Biol.* **40** 4109-18